Publ. Astron. Inst. ASCR 93, 36 – 43 (2005)

Long Baseline Interferometry of Be Stars

A Basic Introduction and First Results from MIDI/VLTI

O. Chesneau[1,2], Th. Rivinius[3]

[1] *Max-Planck-Institut für Astronomie, Königstuhl 17, 67117, Heidelberg, Germany; chesneau@mpia-hd.mpg.de*
[2] *Observatoire de la Côte d'Azur, Département Gemini UMR 6203, Avenue Copernic, F-06130 Grasse, France*
[3] *Landessternwarte Königstuhl, 69117 Heidelberg, Germany; triviniu@lsw.uni-heidelberg.de*

We give an introduction to interferometrical concepts and their applicability to Be stars. The first part of the paper concentrates on a short historic overview and basic principles of two-beam interferometric observations. In the second part, the VLTI/MIDI instrument is introduced and its first results on Be stars, obtained on α Ara and δ Cen, are outlined.

Keywords: Optical interferometry – Be stars

1 Introduction

In the recent past, optical interferometry has made the greatest impact in the area stellar astrophysics, in particular the study of nearby single stars. Be stars are hot stars that exhibit, or have exhibited the so-called Be phenomenon, i.e. Balmer lines in emission and infrared excess, interpreted as an equatorial disk around these objects. Be stars are relatively frequent among the B-type objects, and therefore, many bright and close Be stars are known.

These stars have been preferred targets for long baseline interferometry since long, and the Be community has followed the new developments of optical long baseline interferometry to study the circumstellar environments of Be stars with great interest (see also the recent review of Stee et al. 2005)

The first environment resolved was the one of γ Cas. Thom et al. (1986) used the I2T for this, and Mourard et al. (1989) saw evidence for a rotating circumstellar environment by inspecting the visibility across the line itself using the GI2T.

These results clearly demonstrated the potential of observations that combine spectral and spatial resolution, but also that extensive modeling is required to interpret measurements obtained with very limited sampling of the *uv*-plane. The first model specialized for this task was the one developed by Stee & de Araujo (1994) and Stee et al. (1995). Their model represents the environment of a Be star as an axisymmetric structure, based on a latitude-dependant radiatively driven wind. The model confirms that its free parameters can be constrained by comparison of predicted line profiles and visibilities.

With a good range of baselines, the Mark III instrument was able to determine the geometrical aspect of seven Be stars, i.e. the axial ratio of their elongated Hα circumstellar emission region (Quirrenbach et al., 1993a, 1994, 1997). The axial ratios r span a wide range, with $r < 0.5$ for ϕ Per, ψ Per and ζ Tau, an intermediate ellipticity ($r = 0.7$) for γ Cas, and $r \sim 1$ for η Tau and 48 Per. In the disk model for Be stars, this can easily be understood as an inclination effect. The strong correlation of the minimum inclination derived in this way with polarimetric estimates supports the geometrically thin-disk hypothesis (Quirrenbach et al. 1997).

The Mark III was specifically designed to perform wide-angle astrometry, but a variable baseline that could be configured from 3m to 31.5m provided the flexibility needed for a variety of astronomical research programs. Mark III was the first interferometer having a full computer control of the siderostats and delay lines which allowed almost autonomous acquisition of stars and data taking. This capability was an important factor for the calibration of instrumental effects and for the scientific productivity of the instrument.

Among the stars investigated with Mark III were also γ Cas and ζ Tau. In their disks asymmetric Hα emission with respect to the central object was later

uncovered with the GI2T instrument. Using spectral Differential Interferometry (DI) it has become possible to monitor such structures of Be disks during a long time (several years) with great spatial resolution (Vakili et al. 1998, Bério et al. 1999).

The field of optical and infrared (IR) interferometry has seen rapid technical and scientific progress over the past decade and the interferometric efficiency improves now dramatically in the era of the Very Large Telescope Interferometer (VLTI). The design of ESO's VLTI, which is the first large optical/IR telescope facility expressly designed with aperture synthesis in mind, is of a hybrid type: There are the four large 8.2 meter spatially fixed unit-telescopes, but additionally there will be four auxiliary telescopes of smaller, i.e. 1.8-meter aperture, which can be moved and set up at a large number of locations. Three recombiners are attached to this structure: VINCI was foreseen to be a K band test instrument but has provided such precise visibility measurements that numerous outstanding science results have been published from its observation. MIDI is the first direct recombiner operating in N band in the world, which is described extensively in the following. Finally, AMBER, currently being in commissioning phase, is an impressive three-beam spectro-interferometer operating in J, H and K bands with a spectral resolution reaching 10 000.

A challenge for the understanding of the Be star phenomenon is the rapid increase of our knowledge of the central star itself. Be stars are statistically rapid rotators and subject to a strong von Zeipel effect (1924). In 2001, van Belle et al. (2001) observed Altair (HD 187642, A7V) using two baselines of the Palomar Testbed Interferometer (PTI). They calculated the apparent stellar angular diameters from measured squared visibility amplitudes using the uniform-disk model and found that the angular diameters change with position angle. This was the first measurement of stellar oblateness owing to rapid rotation. In parallel, the observable consequences of this effect on the interferometric observation have been extensively studied by Domiciano de Souza et al. (2002) under the Roche approximation (uniform rotation and centrally condensed star). Two effects are competing affecting the interferometric signal: the geometrical distortion of the stellar photosphere and the latitudinal dependence of the flux related to the local gravity resulting from the von Zeipel theorem. The measurements from the PTI were not sufficient to disentangle between these two effects but recent observations using closure phases[1] from the NPOI interferometer reported in Ohishi et al. (2004) have confirmed the oblateness of the star and have evidenced a bright region attributed to the pole. The observations of Altair from PTI, NPOI and also from VLTI/VINCI cover now three spectral regions visible, H and K band and an extensive modeling of the star has been undertaken by A. Domiciano de Souza.

Altair is still a relatively cool and small star compared to the Be stars and its gravity surface remains large, therefore larger effects of the rotation are expected for Be stars. In 2003, the large oblateness of the Be star Achernar (α Eri) was measured with VLTI/VINCI (Domiciano de Souza et al. 2003). The measured oblateness of 1.56±0.05 based on equivalent Uniform Disk apparently exceeds the maximum distortion allowed in the Roche approximation and no models investigated by Domiciano de Souza et al. (2002) could be satisfactorily fitted to the observations. These observations open a new area for the study of the Be phenomenon and VLTI/AMBER should take over this study and expand rapidly the number of target observed.

Recently, VLTI/MIDI observed two Be stars, α Ara (B3 Ve) and δ Cen (B2 IVne) from 8 to 13 μm with baselines reaching 100 m but their circumstellar environment could not be resolved. These observations are also reported in this paper.

2 Basic Principles of Stellar Interferometry

This section will review the basic principles of stellar interferometry. More detailed discussions of optical interferometry issues can be found in the reviews by Monnier (2003) and by Quirrenbach (2001). In order to introduce the principles, we restrict ourselves to the case of a single interferometric baseline, i.e. with two telescopes only. We adopt the formalism of Domiciano de Souza et al. (2002) and reproduce here the equations necessary for an introduction to natural light interferometry.

2.1 Basic principles

Let us consider an astrophysical target located at the center of a Cartesian coordinate system (x, y, z). The system is oriented such that the y axis is defined as the North-South celestial orientation and the x axis points towards the observer.

Next, we define the sky-projected monochromatic brightness distribution $I_\lambda(y, z)$, hereafter called "intensity map". Interferometers measure the complex visibility, which is proportional to the Fourier transform of $I_\lambda(y, z)$, which shall be denoted $\widetilde{I}_\lambda(y, z)$. The complex visibility in natural light can then be written

[1] Closure phases are measured when at least three telescopes are operating simultaneously.

as:

$$V(f_y, f_z, \lambda) = |V(f_y, f_z, \lambda)|\, \mathrm{e}^{\mathrm{i}\phi(\mathrm{f_y},\mathrm{f_z},\lambda)} \quad (1)$$

$$= \frac{\widetilde{I}_\lambda(f_y, f_z)}{\widetilde{I}_\lambda(0,0)} \quad (2)$$

where f_y and f_z are the Fourier spatial frequencies associated with the coordinates y and z. These spatial frequencies in long-baseline interferometry are given by $\vec{B}_{\rm proj}/\lambda_{\rm eff}$, where $\lambda_{\rm eff}$ is the effective wavelength of the spectral band considered and $\vec{B}_{\rm proj}$ is a vector representing the baseline of the interferometer projected onto the sky. The vector $\vec{B}_{\rm proj}$ defines the direction s, which forms an angle ξ with the y axis so that

$$\vec{B_{\rm proj}} = (B_{\rm proj}\cos\xi)\,\widehat{y} + (B_{\rm proj}\sin\xi)\,\widehat{z} \quad (3)$$

where $\widehat{y}$ and $\widehat{z}$ are unit vectors. Note that *large* structure in image-space results in *small* structure in Fourier transformed, i.e. visibility-space.

We consider linear cuts along the Fourier plane corresponding to a given baseline direction $\widehat{s}$. Then we can define the new spatial frequency coordinates (u, v) for which $\vec{B}_{\rm proj}$ is parallel to the unit vector $\widehat{u}$. In that case the line integral (or strip intensity) of $I_\lambda(s, p)$ over p for a given ξ can be written as:

$$\widetilde{I}_{\lambda,\xi}(u) = \int I_{\lambda,\xi}(s)\mathrm{e}^{-\mathrm{i}2\pi\mathrm{su}}\mathrm{ds} \quad (4)$$

The *complex visibility* is given by:

$$V_\xi(u,\lambda) = |V_\xi(u,\lambda)|\,\mathrm{e}^{\mathrm{i}\phi_\xi(\mathrm{u},\lambda)} = \frac{\widetilde{\mathrm{I}}_{\lambda,\xi}(\mathrm{u})}{\widetilde{\mathrm{I}}_{\lambda,\xi}(0)} \quad (5)$$

By varying the spatial frequency (meaning the baseline length and/or wavelength), we obtain the so-called visibility curve. Eqs. 4 and 5 say that the interferometric information along $\vec{B}_{\rm proj}$ is identical to the one-dimensional Fourier transform of the curve resulting from the integration of the brightness distribution in the direction perpendicular $(\widehat{p})$ to this baseline. The interferometric observable, called visibility is directly related to the fringe contrast.

The visibility can be observed either as the fringe contrast in **an image plane** (as with AMBER) or by modulating the internal delay and detecting the resulting temporal variations of the intensity in a pupil plane (as done with VINCI or MIDI).

It should be stressed that the signal-to-noise ratio (SNR) of interferometric observables depends not only on the photon count N, but on NV^2 for the photon-noise limited regime (optical) and on NV for the background-limited regime (MIDI). Indeed, the interferometer is not sensitive to the total flux from the source but to the *correlated* one.

In Fig. 1 we show several examples of intensity maps and their corresponding visibility curves, depending on the baseline orientation. All models, except the binary, are symmetrical which means that the interferometer will provide the same visibility for a particular baseline length (projected onto the sky), whatever its direction. The second model shows the visibility curves from a binary system, consisting of two stars of the same diameter. In the case where the baseline is perpendicular to the binary's position angle, the interferometer is unable to distinguish the two components and sees a visibility signal close to the one provided by a single uniform disk. When the baseline is aligned with the binary's PA, the binary signature is superimposed to the signature from the individual components.

The uniform ring structure is an interesting intermediate situation between the uniform disk and a binary. The interferometer sees mainly a binary structure and owing to the symmetry of the source, this signal is the same whatever the baseline direction. This example could appear quite artificial, yet it reflects a geometry which can be encountered frequently in the inner rims of a Young Stellar Objects and even more evolved star's disks.

Finally, we show the example of an object exhibiting a Gaussian distribution of light, like approximating a circumstellar environment with outwards decreasing emission. The Fourier transform of a Gaussian being a Gaussian too, the visibility curve will not show the characteristic lobes which are seen in the other curves. It must be stressed out that these lobes are the consequence in the Fourier domain of a discontinuity of the light distribution in the image plane. For instance, a limb-darkened disk will exhibit a visibility curve with the lobes attenuated compared to the uniform disk case. One can, in fact, note a small lobe in the Gaussian visibility curve in Fig. 1. This is the consequence of the numerical truncation of the Gaussian, generating a discontinuity at the limit of the chosen Field-of-View.

Of course, for typical main sequence stars, this implies long baselines and it must be stressed that at this stage the contrast of the fringes is so low that this experiment is very demanding in terms of signal-to-noise ratio, i.e. in terms of target flux.

2.2 Differential Interferometry (DI)

Differential Interferometry (DI) uses the high angular resolution interferometric capabilities in a dispersed mode in order to compare the spatial properties of an object at different wavelengths (Vakili et al. 1994, 1997, 1998). This technique offers obvious advantages: over few nanometers, the (differential) atmospherical turbulence effects are negligible, and the differential sensitivity can be much better than expected by classical techniques. In interferometry, an unresolved source is required for calibration, and such an object can be difficult to find. In particular cases, such as Be stars, the continuum can be regarded as

Visibility and phase as observational concepts

Interference pattern of a monochromatic point-source

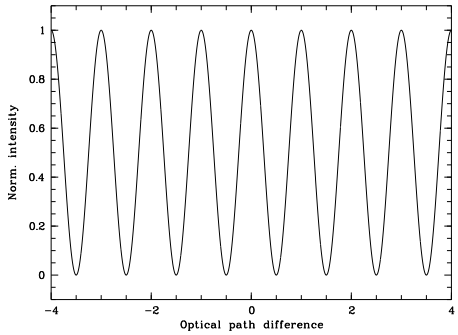

Polychromatic point-source

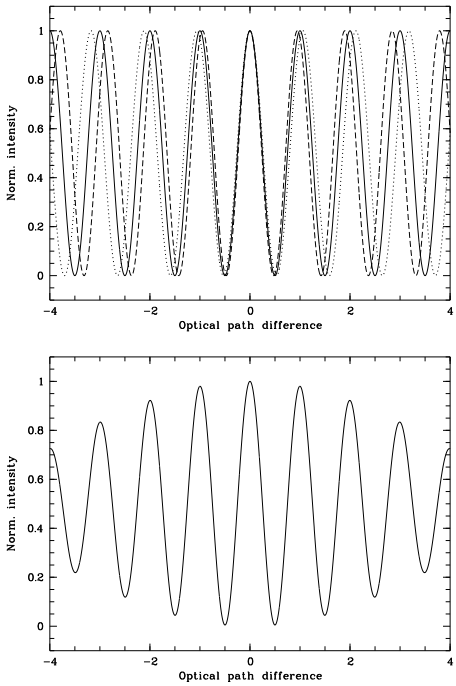

The interference patterns of the various colours add up to a spatial modulation of the pattern. Note that the amplitude at OPD=0, the "white-light fringe" is still at maximum

Monochromatic extended source

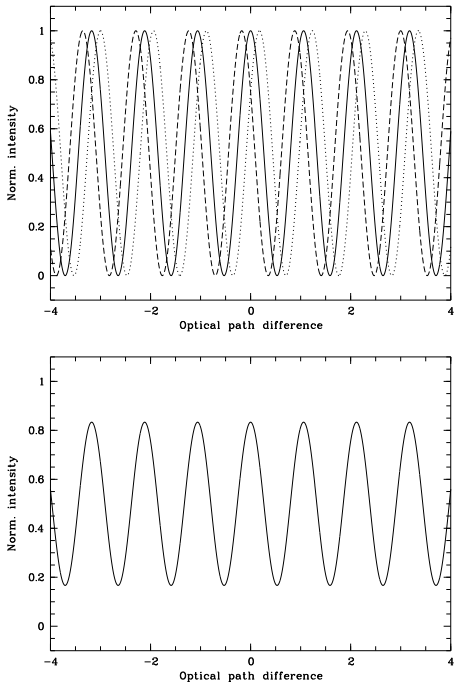

The interference patterns from the local points add up to a pattern of reduced amplitude, independent of the optical path difference (OPD), however.

Both principles combined give the fringe patterns as seen by interferometry. The "visibility", holding the spatial extend of the investigated source is quantifying the amplitude, as in the right column. Suppose a source observed at two different wavelengths, one can obtain *relative* positional information by measuring whether the OPD for maximal positive interference has shifted. This concept is called "interferometric phase"

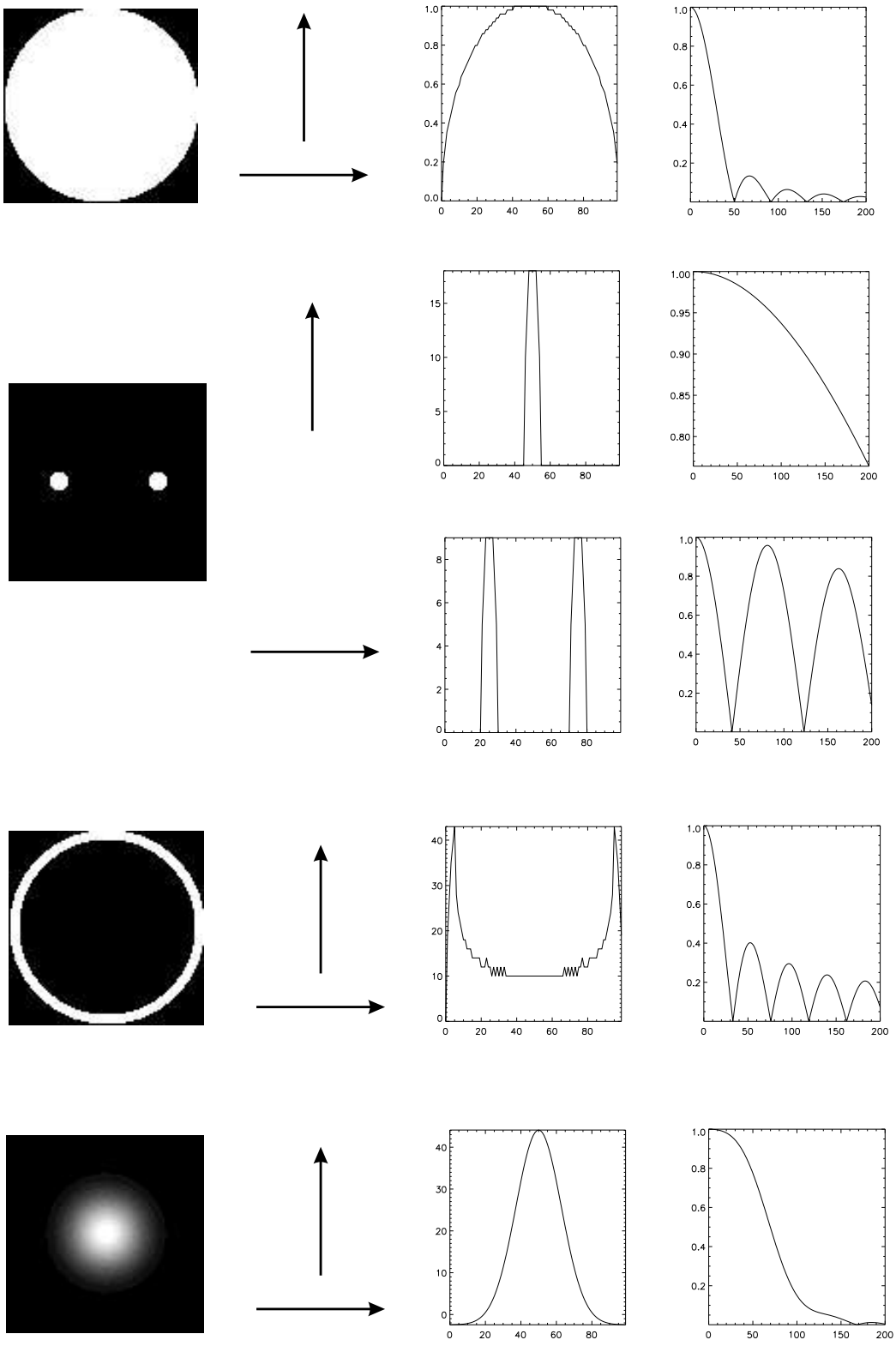

Figure 1: In this figure typical examples of intensity maps (left) are shown. From top to bottom these are a uniform disk, a resolved binary, a ring and a Gaussian distribution. The models are "observed" with a horizontal ad vertical baseline. The 1-D flux intensity along the baseline is shown in the middle and the corresponding visibility is displayed on the right. All units are arbitrary. A further description of visibility curves is given in the text.

unresolved, whereas emission lines emitted by an extended circumstellar environment are angularly resolved. Moreover, the continuum can be considered as a *polarization* reference in the Zeeman effect context.

The phase of the visibility is generally lost due to the blurring effect of the atmosphere, but DI can retrieve a *relative* spectral phase. Some algorithms can compare the properties of the fringes studied in a (broad, i.e. continuum) reference spectral channel at wavelength λ_r with the ones in a (narrow, i.e. spectral line) science channel at wavelength λ_s. This can be performed by means of cross-correlation of a broad continuum channel with a series of narrow channels across the emission line as encountered in Be stars. These steps are then repeated with small wavelength shifts for both channels from the blue to the red wing of the line, starting and finishing in the continuum next to the line on both sides. Since the signal to noise ratio in the cross-correlations depends on the geometric mean of the number of photons in channel r and channel s, the interferometric signal can be safely estimated in the narrow channel even if the flux or the fringe visibility are very small in this channel.

The accuracy of the phase determination, which allows to measure a position can be better than the actual resolution of the interferometer, but again the super-resolution power of cross-spectral density methods apply, as long as the star is partially resolved (Chelli & Petrov 1995). For instance, a positive (negative) relative phase indicates the position at the north (south) of the central star if the baseline is oriented North-South. The relative phase shift between to spectral channels is related to the photocenter of the object by the following first order equation:

$$\phi(\vec{u}, \lambda_r, \lambda_s) = -2\pi\vec{u}.[\vec{\epsilon}(\lambda_s) - \vec{\epsilon}(\lambda_r)]$$

Using the continuum fringes as reference for the phase one can, for instance, determine whether the light distribution in a spectral line is centered on this continuum, as any departure from symmetry, e.g. due to localized circumstellar emission or a magnetic field, causes a spectral phase effect. While the visibility is a quadratic estimator, the phase sensitivity depends linearly on the photon count.

Increasing theoretical predictions of photocenter positions through emission or absorption lines are available concerning the environment of stars (Stee et al. 1996, Dessart & Chesneau 2002) or the study of the underlying photosphere (Domiciano et al. 2002, 2004).

3 MIDI Interferometer

MIDI is the first 10 μm interferometric instrument worldwide using the full available atmospheric transmission window. Due to the MIR radiation of the environment and the optical setup itself, most of the instruments optics is inside a dewar and is cooled to cryogenic temperatures. The incoming afocal VLTI beams are combined on the surface of a 50:50 beam splitter, which is the heart of the instrument. Spectral information from 8 μm to 13.5 μm can be obtained by spectrally dispersing the image using a prism for low (R=30), or a grism for intermediate (R=270) spectral resolution. For source acquisition a field of 3" is available. This small area on the sky represents about 10 times the Airy disk of a single UT telescope. This field is useful especially in case of extended objects like the S Doradus variable (also called LBV) η Car (Chesneau et al. 2005a) or some Herbig stars (like HD 100 546, Leinert et al. 2004).

MIDI measures the degree of coherence between the interfering beams (i.e. the object visibility) by artificially stepping the optical path difference between the two input beams rapidly, using its internal delay lines. The result is an intensity signal modulated with time from which the fringe amplitude can be determined. The total (uncorrelated) flux is determined separately by chopping between the object and an empty region of the sky, and determining the source flux by subtraction. In this mode MIDI is working like an usual mid-infrared camera. An example of a resulting image in case of the observation of η Carinae is shown in Chesneau et al. (2005a) which demonstrates the excellent imaging capabilities of the MIDI/VLTI infrastructure, even if it sends the light via 31 mirrors and 5 transmissive elements until it reaches the detector.

Observing with an interferometer requires accurate preparation. Useful tools for that are simulation programs like ASPRO (by the Jean-Mariotti Center, Fr.), SIMVLTI (by the MPIA Heidelberg, Ge.) or ESO's VLTI visibility calculator. Those software packages make it possible to get an idea of the expected visibility values for given parameter setups. For further reference, the reader should also consult the MIDI web page at ESO[2].

When planning observations with MIDI, a few constraints have to be kept in mind. Of course, the object should be bright enough in the mid-IR to be measured with MIDI. However, for self-fringe tracking, the source not only has to be bright enough in total, but there must be sufficient flux concentrated in a very compact ($< 0.1''$) central region, to which then the interferometric measurements will refer. Also, the *visual brightness* should be at least 16 mag, in order to allow the operation of the MACAO tip-tilt and adaptive optics system.

In addition, one has to consider that interferometry with two telescopes of the VLTI in a reasonable

[2] http://www.eso.org/instruments/midi/

time of several hours will provide only few measured points of visibility, i.e. only a few points where the Fourier transform of the object image is determined. The scientific programme has to be checked before whether its main questions can be answered on this basis (e.g. to determine the diameter of a star one does not need to construct an image of its surface).

4 Be stars observed by MIDI

4.1 α Ara

The first VLTI/MIDI observations of the Be star α Ara show a nearly unresolved circumstellar disk in the N band (Chesneau et al. 2005b). α Ara (HD 158 427, B3 Ve) is one of the closest Be star with an estimated distance of 74pc±6pc, based on the Hipparcos parallax, and color excesses E(V-L) and E(V-12 μm) among the highest of its class. The interferometric measurements made use of the UT1-UT3 projected baselines of 102 m and 74 m, at two position angles of 7° and 55°, respectively. The object is mostly unresolved, putting an upper limit to the disk size in the N band of the order of $\phi_{\rm max} = 4$ mas, i.e. 14 $R_\star$ at 74 pc and assuming $R_\star = 4.8 R_\odot$, based on the spectral type.

On the other hand, the density of the disk is large enough to produce strong Balmer emission lines. The SIMECA code developed by Stee (1995) and Stee & Bittar (2001) has been used for the interpretation. Optical spectra from the HEROS instrument, taken 1999, when the instrument was attached to the ESO-50cm telescope, and infrared ones from the 1.6m Brazilian telescope have been used together with the MIDI visibilities to constrain the system parameters. In fact, these two observations, spectroscopy vs. interferometry, put complementary constraints on the density and geometry of the α Ara circumstellar disk. It was not possible to find model parameters that at the same time are able to reproduce the observed spectral properties, both in the emission lines and in the continuum flux-excess, and the interferometric null-result, meaning that the disk must be smaller than 4 mas.

However, the Hydrogen recombination line profiles of α Ara exhibit (quasi?)-periodic short-term variations of the violet-to-red peak heights of the emission profiles (V/R-variability, see Mennickent & Vogt, 1991 and this study). The radial velocity of the emission component of the Balmer lines changes in a cyclic way as well in these lines. This may point to a possible truncation of the disk by a putative companion, that could explain the interferometric observations.

Using the NPOI interferometer, Tycner et al. (2004) have recently studied the disk geometry of the Be star ζ Tau, which is also a well-investigated spectroscopic binary (P∼133d, K∼10 km s^{-1}). They measured the disk extension quite accurately to be well within the Roche radius. This suggests also that this disk may be truncated.

4.2 δ Cen

δ Cen (HD 105 435, B2 IVe, $F_{12\mu m}$=15.85 Jy), situated at about 120 pc, is one of the very few Be stars which has been detected at centimeter wavelengths (Clark et al. 1998) and also the only star for which significant flux has been measured at 100μm (Dachs et al. 1988). These two measurements suggest an extended disk, contrary to the case of α Ara.

However, recent VLTI/MIDI observations of δ Cen during Science Demonstration Time (programme conducted by D. Baade) with a baseline of 91 m have not been able to resolve the disk of this object as well. It must be stressed out that these observations have been conducted under much better atmospheric conditions than those for α Ara, leading to a well constrained upper limit of 4±0.5 mas for the equivalent Uniform Disk diameter.

This is roughly the same size as was determined for other Be stars using interferometry in the wavelength region of Hα. Note that for these Hα observations the baseline was much less than the one used here, about 40 m vs. 100 m. That both datasets still come up with the same angular resolution is due to the scaling of the spatial frequency with the effective wavelength introduced in Sect. 2.1.

Whether or not a Be star disc should be resolved in the near IR depends on the model one adopts for such a disk. Based on modelling of the Balmer-line emission, at least one model does predict a resolved disk, while others don't (see Chesneau et al., 2005, for a detailed discussion). In this sense, even null-results provide important constraints to our understanding of Be star disks.

5 Conclusions

Although being null-results these observations, as others before, have shown the potential discriminating power of interferometric observations for the current open questions of Be star research.

Long baseline interferometry is now able to provide a complete set of observations from the visible to the thermal infrared at high angular and spectral resolution, opening a new area for the study of the Be phenomenon. In particular, this technique is now able to study the complex interplay between fast rotator distorted photospheres, affected by the von Zeipel effect and their direct surroundings by means of spectrally resolved NIR observations and MIR ones. The

Guaranteed Time Document of the VLTI/AMBER[3] gives a good idea of the possibilities opened by this new instrument.

The first VLTI/MIDI observations of Be stars have demonstrated the need to use long baseline at these wavelengths in order to resolve the disk of even the few closest (and brightest) Be stars. The VLTI 1.8 m Auxiliary Telescopes (ATs) AT1 and AT2 are currently being commissioned at Paranal observatory and should be able to observe their first fringes in mid-2005. The ATs are movable telescopes which can project onto the sky a baseline from 8 to 200 m. Such long baselines should be perfectly suited for MIDI to study the inner disk of Be stars, and for AMBER to observe the star itself, whereas the shorter ones would allow AMBER to study the close environment from the photosphere to several stellar radii.

References

Bério P., Stee Ph., Vakili F., et al.: 1999, A&A 345, 203

Chelli A., Petrov R. G.: 1995, A&AS 109, 389

Chesneau O., Min M., Herbst T., et al.: 2005a, A&A 435, 1043

Chesneau O., Meilland A., Stee Ph., et al.: 2005b, A&A 435, 275

Clark J. S., Steele I. A., Fender R. P.: 1998, MNRAS 299, 1119

Dachs J., Engels D., Kiehlin R.: 1988, A&A 194, 167

Dessart L., Chesneau O.: 2002, A&A 395, 209

Domiciano de Souza A., Vakili F., Jankov S.: 2002, A&A 393, 345

Domiciano de Souza A., Kervella P., Jankov S., et al.: 2003, A&A 407, L47

Domiciano de Souza A., Zorec J., Jankov S., et al.: 2004, A&A 418, 781

Leinert Ch., van Boekel R., Waters L. B. F. M.: 2004, A&A 423, 537

Monnier J.: 2003, Rep. Prog. Phys. 66, 789

Mourard D., Bosc I., Labeyrie A., et al.: 1989, Nature 342, 520

Ohishi N., Nordgren T. E., Hutter D. J.: 2004, ApJ 612, 463

Quirrenbach A.: 2001, Ann. Rev. Astron. Astrophys. 39, 353

Quirrenbach A., Bjorkman K. S., Bjorkman J. E., et al.: 1997, ApJ 479, 477

Quirrenbach A., Buscher D. F., Mozurkewich D.: 1994, A&A 283, L13

Quirrenbach A., Hummel C. A., Buscher D. F., et al.: 1993, ApJ 416, L25

Stee P.: 1996, A&A 311, 945

Stee P., de Araújo F. X.: 1994, A&A 292, 221

Stee P., de Araújo F. X., Vakili F.: 1995, A&A 300, 219

Stee P., Meilland A., Berger D., Gies D.: 2005, ASP Conf. Ser. 337, 211

Thom C., Granes P., Vakili F.: 1986, A&A 165, L13

Tycner C., Hajian A. R., Armstrong J. T., et al.: 2004, AJ 127, 1194

Vakili F., Mourard D., Stee P., et al.: 1998, A&A 335, 261

Vakili F., Mourard D., Bonneau D.: 1997, A&A 323, 183

Vakili F., Bonneau D., Lawson P. R.: 1994, SPIE 2200, 216

van Belle G. T., Ciardi D. R., Thompson R. R., et al.: 2001, ApJ 559, 1155

von Zeipel H.: 1924, MNRAS 84, 665

[3] available at http://www-laog.obs.ujf-grenoble.fr/amber/